

VERTICAL KINK OSCILLATION OF A MAGNETIC FLUX ROPE STRUCTURE IN THE SOLAR CORONA

S. KIM¹, V. M. NAKARIAKOV^{2,3,4}, AND K.-S. CHO¹

¹ Korea Astronomy and Space Science Institute, Daejeon 305-348, Korea; sjkim@kasi.re.kr

² Centre for Fusion, Space & Astrophysics, Physics Department, University of Warwick, Coventry, CV4 7AL, UK

³ School of Space Research, Kyung Hee University, Yongin, 446-701 Gyeonggi, Korea

⁴ Central Astronomical Observatory of the Russian Academy of Sciences at Pulkovo, 196140 St. Petersburg, Russia

Received 2014 September 3; accepted 2014 November 18; published 2014 December 4

ABSTRACT

Vertical transverse oscillations of a coronal magnetic rope, observed simultaneously in the 171 Å and 304 Å bandpasses of the Atmospheric Imaging Assembly on board the *Solar Dynamics Observatory* (*SDO*), are detected. The oscillation period is about 700 s and the displacement amplitude is about 1 Mm. The oscillation amplitude remains constant during the observation. Simultaneous observation of the rope in the bandpasses corresponding to the coronal and chromospheric temperatures suggests that it has a multi-thermal structure. Oscillatory patterns in 171 Å and 304 Å are coherent, which indicates that the observed kink oscillation is collective, in which the rope moves as a single entity. We interpret the oscillation as a fundamental standing vertically polarized kink mode of the rope, while the interpretation in terms of a perpendicular fast wave could not be entirely ruled out. In addition, the arcade situated above the rope and seen in the 171 Å bandpass shows an oscillatory motion with the period of about 1000 s.

Key words: instabilities – Sun: corona – Sun: evolution – Sun: oscillations

Online-only material: animation, color figures

1. INTRODUCTION

Transverse oscillations of the plasma structures of the solar corona have been subject to intensive investigation for several decades since their first detection in the Doppler shift (Koutchmy et al. 1983) and in EUV intensity (Aschwanden et al. 1999; Nakariakov et al. 1999). These oscillations, confidently interpreted as a standing kink (also known as $m = 1$ in cylindrical geometry) magnetohydrodynamic (MHD) mode, are characterized by a quasi-periodic displacement of the wave-guiding plasma nonuniformity in the direction perpendicular to its axis and hence to the field. The phase speed of a long-wavelength kink mode, the kink speed, is determined by the Alfvén speeds inside and outside the nonuniformity. The kink speed is independent of the plasma temperature for a fixed density. Usually, kink oscillations are seen in EUV loops and in prominence fibrils. Detected periods range from tens of seconds (e.g., Koutchmy et al. 1983; Kupriyanova et al. 2013b) in the white light and microwave bands to several minutes (e.g., Aschwanden et al. 1999; Nakariakov et al. 1999) and up to several hours (Hershaw et al. 2011) in the EUV band. In the vast majority of cases, horizontally polarized oscillations are seen. Only in a few cases was clear evidence found of vertically polarized oscillations in the EUV (Wang & Solanki 2004; White et al. 2012; Srivastava & Goossens 2013) and microwave (Kupriyanova et al. 2013a) imaging data.

Kink oscillations appear in two different regimes, the high-amplitude, rapidly decaying oscillations and the low-amplitude oscillations without decay (Nisticò et al. 2013). In the former regime, the displacement amplitude reaches several millimeters, which is equal to several widths of the oscillating structure, e.g., several minor radii of the oscillating loop (see, e.g., De Moortel & Nakariakov 2012). The decay usually occurs in a few periods of the oscillation and is interpreted as the transfer of the energy of the collective kink motion to unresolved torsional Alfvénic oscillations. This transfer can occur if there is a

smooth profile of the Alfvén speed across the wave-guiding non-uniformity. There have also been alternative mechanisms proposed, e.g., phase mixing (Ofman & Aschwanden 2002; Ofman 2009), and interference fringes resulting from impulsive driving of an arcade of field lines (Hindman & Jain 2014). In the latter regime, the displacement amplitude is less than a few millimeters. Several cycles of the oscillations are usually seen without any noticeable decrease in the apparent amplitude. The nature of the regime without decay has not yet been revealed.

The main interest in kink oscillations is connected with the diagnostics of the absolute value of the magnetic field (e.g., Nakariakov & Ofman 2001), density scale height (e.g., Arregui et al. 2007), vertical variation of the magnetic field (e.g., Verth & Erdélyi 2008), sub-resolution spatial structuring (Van Doorselaere et al. 2008), and with the coronal heating problem (e.g., Goossens et al. 2013).

On a much larger scale, periodic variations of the outward speed of coronal mass ejections (CME) are also associated with the transverse oscillations of magnetic flux ropes (Krall et al. 2001; Shanmugaraju et al. 2010). The oscillations are seen at distances of 3–25 solar radii from the Sun. The observed periods range from one to several hours. It is interesting that these oscillations are vertically polarized, which makes them different from the horizontally polarized oscillations usually observed in the lower corona. It was proposed that the CME speed oscillations are produced by the combination of the aerodynamic drag force that either accelerates or decelerates the CME depending on whether it propagates slower or faster than the solar wind speed (Shanmugaraju et al. 2010) and the magnetic force (Cargill et al. 1994).

In this Letter, we report vertical oscillations of a plasma rope observed at a much lower height, below 1.2 solar radii. Thanks to the Atmospheric Imaging Assembly (AIA; Lemen et al. 2012) on board the *Solar Dynamics Observatory* (*SDO*), which monitors the entire Sun with high spatial resolution, high time-cadence, and several EUV channels, the detailed evolution

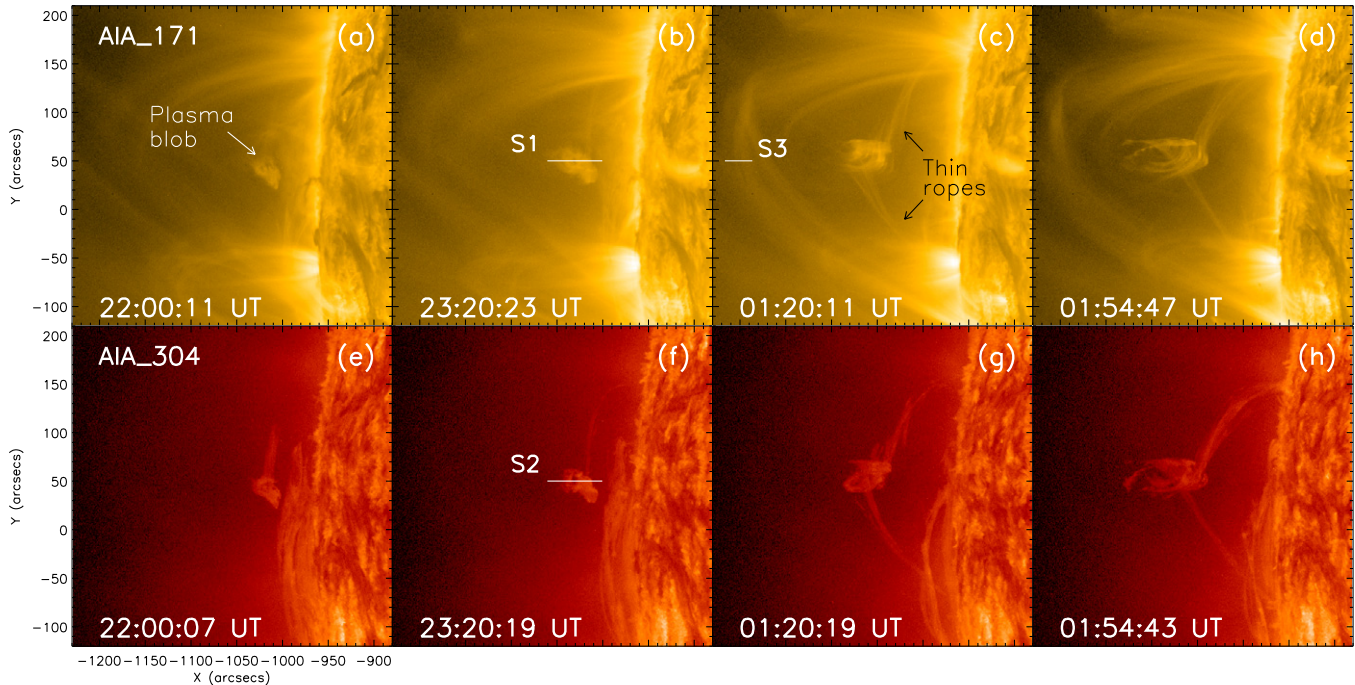


Figure 1. Evolution of the plasma blob and associated thin ropes observed by the AIA 171 (upper row) and 304 channels (lower row). The sequential images show that the morphology of the plasma blob and thin ropes evolves into a kinked rope. White lines crossing the blob (S1 and S2) and the overlying field (S3) are slits to examine the time-space plot.

(An animation and a color version of this figure are available in the online journal.)

of such a structure with has weak emissivity and which takes place in the quiet region could be discovered. An overview of the observations is presented in Section 2. The detection of the oscillation and its properties are described in Section 3. Our conclusions are summarized in Section 4.

2. OVERVIEW OF THE EVENT

The plasma blob discussed in this Letter appeared above the Eastern limb of the Sun around 21:00 UT on the 2014 April 14, and disappeared at around 03:00 UT on 15 April. Later on, close to the site of this event, the NOAA active region 12042 developed. There were no significant flares during the time interval of interest. There was a weak CME at around 19:00 UT observed by *SOHO*/LASCO C2 (16 hr after the rise of the plasma blob). There was also a back-side event observed by *STEREO-B* at around 13:00 UT. Thus, there was no CME that corresponded to the blob eruption. It is clear that the event was a failed eruption.

The AIA 171 Å and AIA 304 Å channels reveal a quite well-pronounced isolated structure of a bright blob situated off-limb and its evolution. The 171 Å channel predominantly includes the emission from the Fe IX line that formed at 0.6 MK, and the 304 Å channel has predominant emission from the He II line that formed at 0.05 MK (Boerner et al. 2012). The AIA provides imaging data with a spatial resolution of 0.6 per pixel every 12 s. Apparently, the blob is a view of a magnetic rope filled with a dense plasma seen from the butt-end.

Figure 1 shows the evolution of the blob in the 171 Å (top) and 304 Å channels (bottom). In the 171 Å channel, a bright plasma blob is formed above the solar surface at about 22:00 UT (Figure 1(a)), and then gradually rises upward with a repetitive vertical motion (Figure 1(b); see also the animation). At about 01:20 UT, thin bright ropes linking the blob to the solar surface come into sight (Figure 1(c)). At about 01:54 UT, the upper

part of the blob rapidly moves up with the ascendance of whole structure (Figure 1(d)). A large bundle of bright loops situated above it is seen to expand upward together with the motion of the blob. Eventually, the plasma blob fades away and disappears from sight. The blob is also clearly seen in the 304 Å channel. The sequential images of the blob’s evolution seen at 304 Å (Figures 1(e)–(h)) show progress consistent with that seen at 171 Å except for the absence of the bundle of bright loops above the blob. The similarity of the blob evolution seen in the 171 Å and 304 Å channels indicates that the plasma blob comprises multi-thermal structures covering the chromospheric to coronal temperature range. The linear length between the footpoints of the thin ropes is estimated as 200'', while the height of the blob above the limb is about 90''. Thus, we assume that the blob central axis has a circular shape with a diameter of 190'' and an estimate of the length of the magnetic rope of about 300'' or about 220 Mm. The projection effects can increase this estimation. On the other hand, the height of the bundle of the 171 Å loops was around 230''. Assuming a semi-circular shape of the bundle, we estimate its length to be about 530 Mm.

Figures 1(d) and (h) show that the ascending plasma blob consists of several curved threads. The individual threads are well seen in both the 171 Å and 304 Å channels. Assuming that the observed blob is a twisted magnetic rope, we take the thin ropes linking the blob with the solar surface to be continuations of the magnetic threads that form the blob. The plasma can flow up and down along the field-aligned threads. Consideration of the mass and energy balance in the observed rope is beyond of scope of this study.

3. DETECTION OF THE OSCILLATIONS

We apply the standard method of the time–distance plot for the measurements of the parameters of the kink oscillations of the blob. The time–distance plots (see Figure 2) are made

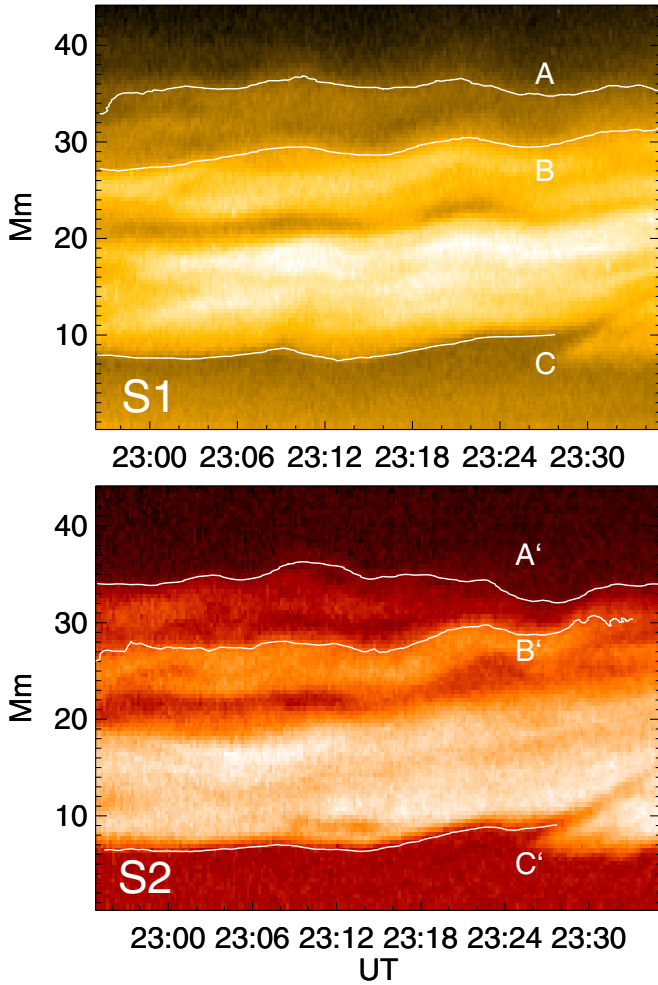


Figure 2. Time-space plots of the slits S1 (AIA 171) and S2 (AIA 304) denoted in Figures 1(b) and (f), respectively. These slits are crossing the center of the plasma blob vertically. Wavy patterns with white curves are extracted from the intensity contour.

(A color version of this figure is available in the online journal.)

along vertical slits S1 (Figure 1(b)) and S2 (Figure 1(f)) passing through the blob. The oscillation of interest co-exists with other dynamical processes and the time and spatial scales are different from the period and wavelength of the oscillation, which contaminates the observation. To optimize the detection, the slits are taken to be 6 pixels wide for S1 and 7 pixels wide for S2 in the horizontal direction. The slits have the same location in the 171 Å and 304 Å images. The time–distance plots demonstrate that the blob periodically gets displaced in the vertical direction. We traced the wavy patterns by following the variation of the spatial positions of the constant brightness in the blob, shown by curves A, B, and C in 171 Å and A', B', and C' in 304 Å (see Figure 2). Positions A and B and A' and B' are chosen at the top of the slope at the front of the blob, and positions C and C' are at the bottom of the slope behind the blob.

The curves showing the time variation of positions A, B, and C and A', B', and C' have a clear oscillatory pattern without decay. In order to subtract the rising motion of the blob from the original curves, we obtained quasi-linear trends by smoothing the original curves for 10 minutes. Then the original signals were detrended. The oscillatory patterns were clearly seen in the detrended signals. The obtained signals were approximated

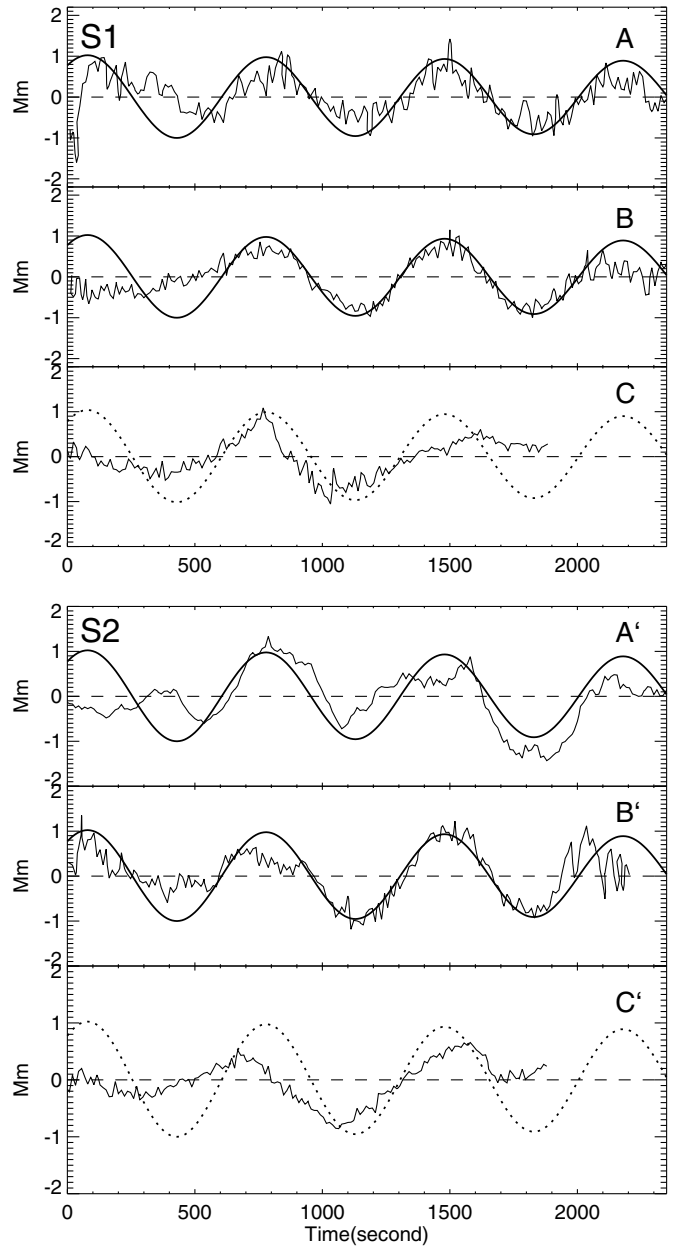


Figure 3. Detrended oscillating patterns of S1 and S2 by their smoothed curves (thin line) and best-fit (thick line). Detrended oscillating patterns for S1 and S2 of Figure 2. Top panel: three top panels from show the oscillations in the upper (A), middle (B), and bottom (C) parts of the plasma blob in S1 (AIA 171 channel). Thick lines and the dotted line are the best fits for contour A of S1. Bottom panel: the oscillating pattern in S2 (AIA 304 channel). The best-fitting curve for contour A of S1 is drawn with a thick line.

by a harmonic function

$$s(t) = A \sin(2\pi t/P + \phi_0), \quad (1)$$

where s is the position along the slit at time t , and A , P , and ϕ_0 are the amplitude, period, and initial phase of the oscillation. Parameters of the best-fitting harmonic functions were determined by the least squares error method.

Figure 3 presents the results of the approximation that show a fairly good agreement between the data and the best-fitting harmonic function. The oscillation period is found to be about 700 s and the displacement of amplitude is about 1 Mm. The oscillatory displacements of the top and bottom slopes of the blob are mainly in phase. Thus, the oscillation is of the kink

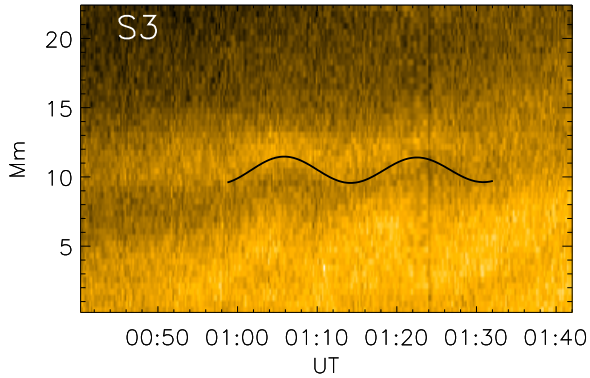


Figure 4. Time-space plot of the slit S3 denoted in Figure 1(c) (AIA 171). A black wavy line is the best-fit of the bright oscillating pattern.

(A color version of this figure is available in the online journal.)

symmetry. The oscillatory patterns seen in 171 Å (S1) and 304 Å (S2) are approximately in phase with the same period and amplitude.

Later on, a similar oscillatory pattern appears in the large bundle of bright loops situated above the blob. The oscillation occurs when the plasma blob rises rapidly at 01:00-01:35 UT. We visualized the oscillation by the time-distance plot (Figure 4) made along the vertical slit S3 positioned across the loop bundle in the 171 Å images (Figure 1(c)). This plot was constructed by the same approach as Figure 2. The best-fitting harmonic pattern with a period of 1000 s and an amplitude of about 1 Mm is shown by the black curve. The low signal-to-noise ratio and the short duration of the detection of the oscillations (only two cycles) do not allow us to establish whether or not the signal is decaying.

4. RESULTS AND CONCLUSIONS

We detected transverse oscillations of a gradually emerging magnetic flux rope. The oscillations are transverse to the local axis of the rope. The oscillations are simultaneously seen in the 171 Å and 304 Å bands, which are associated with the coronal and chromospheric temperatures, respectively. The oscillation period was 700 s. Also, at 171 Å only, a transverse oscillation of a longer period, 1000 s, was detected in a plasma arcade situated above the flux rope. The oscillation of the rope is characterized by the lateral oscillatory movements of the plasma structure around an equilibrium. Both the front and bottom edges of the rope were seen to oscillate in phase. This finding clearly indicates that we observed the kink magnetoacoustic mode of the oscillating structure. The oscillatory movements were directed radially from the solar surface. The oscillation was seen near the apex of the rope. As the plane of the rope was almost parallel to the line-of-sight, we conclude that a rare example of the vertically polarized kink oscillation was found. Moreover, to the best of our knowledge, for the first time a kink oscillation was detected in a magnetic rope filled in with a hot plasma in the lower corona.

The phase speed of the wave can be determined by the length of the oscillating quasi-cylindrical structure, L , and the period P , as $V_{\text{ph}} = 2L/(PN)$, where N is the mode number (e.g., De Moortel & Nakariakov 2012). Taking the rope length of 220 Mm, and the oscillation period of 700 s, we obtain for the fundamental, $N = 1$, mode $V_{\text{ph}}^{\text{rope}} = 628 \text{ km s}^{-1}$. There could be a possibility that the observed oscillation represents a higher mode with a maximum perturbation at the loop top, e.g., $N = 3$. However, for such a mode the phase speed would be

about 200 km s^{-1} , which requires the plasma parameter beta to be greater than unity (e.g., De Moortel & Nakariakov 2012). Also, the observed periodic displacement could be produced by a propagating wave. It is likely to be a wave propagating along the rope, as it should experience reflection from the footpoints and form a standing pattern. However, a wave propagating in the directions perpendicular to the rope could not be entirely ruled out even though it is not observed outside the rope. We conclude that we most likely observe the fundamental mode of the rope, while the interpretation in terms of a perpendicular fast wave should not be excluded.

Taking the length of the loop arcade above the oscillating rope as 530 Mm and an oscillation period of 1000 s, we get $V_{\text{ph}}^{\text{arcade}} = 1,060 \text{ km s}^{-1}$. Both values are well consistent with typical estimations made for kink oscillations of coronal loops observed in the EUV band (e.g., De Moortel & Nakariakov 2012 and references therein).

In our two-dimensional observation, due to the projection effect, it is not possible to resolve the total twist of the rope. However, one may consider a number of curved threads within the plasma blob as the number of turns of the magnetic field. Figure 1(d) shows that there is about four turns (8π) in the plasma blob. Török et al. (2004) have suggested that a flux rope with a force-free field tends to be kink-unstable when the twist exceeds 3.5π with a large aspect ratio of the loop outer radius to the inner radius ~ 5 . However, as the rope does not seem to experience kink instability in our observation, we take as the empirical result that the observed amount of twist is lower than the instability threshold, and that the rope is marginally stable. In particular, it can be connected with our over-estimation of the twist, as different turns could correspond to different threads, and the actual twisting of an individual thread is lower than 8π . Alternatively, the rope can be kink-unstable, but the growth time of the instability is longer than the observed oscillation period. Recent theoretical modeling of long-wavelength kink oscillations of the twisted magnetic flux tubes (e.g., Karami & Bahari 2012; Terradas & Goossens 2012) demonstrated that the twist does not significantly alter the oscillations, and hence we assume that the detected phase speed of the rope oscillation is about the kink speed.

The simultaneous observation of the magnetic rope in the bandpasses corresponding to the coronal temperature, 171 Å, and the chromospheric temperature, 304 Å, indicates that the rope is a bundle of multi-thermal, field-aligned plasma threads. An interesting result is that the plasmas of the different temperatures show an almost coherent oscillation in our observation. In other words, the multi-thermal plasma threads forming the observed rope oscillate as a distinct structure. This result is not trivial, as the threads of different temperatures may have different densities and hence different Alfvén and kink speeds, and periods of fundamental kink modes. Our finding demonstrates that the kink oscillation is a collective phenomenon, in which the multi-thermal magnetic rope oscillates as a single entity.

Theoretical modeling showed that a collective kink mode may not exist in multi-threaded structures in which the threads have different physical properties (Luna et al. 2009; Soler et al. 2009), while it may occur during an initial transitory phase of the oscillation (Terradas et al. 2008). The discrepancy with our observational finding shows that a collective mode may be connected with the twisted geometry of the observed bundle. This conclusion is consistent with the numerical modeling of Ofman & Aschwanden (2002), which demonstrated the collective oscillations of a twisted multithreaded loop.

The oscillation was seen to neither grow nor decay. This behavior is consistent with the recently discovered low-amplitude regime of kink oscillations of the coronal loops without decay (Wang et al. 2012; Nisticò et al. 2013). Moreover, the rope oscillation amplitude, about 1 Mm, is of the same order of magnitude as in the kink oscillations of loops without decay. The nature of these oscillations has not yet been revealed, and our observation should be taken into account in the development of the relevant theory.

The oscillations of the arcade above the rope can be associated with the oscillation of the rope. A possible mechanism is the leakage of the rope oscillation in the vertical direction by the effect of tunneling, theoretically investigated in Verwichte et al. (2006a, 2006b). In this scenario, the leaking periodic fast magnetoacoustic wave excites the arcade oscillations. The difference in the periods (700 s and 1000 s) may indicate that the excitation is out of resonance. However, the fact that the arcade oscillation occurs about 50 min after the rope oscillation is evidence against this interpretation. Thus, we disregard the possible association of these two oscillations and conclude that they are independent of each other.

The observed vertical oscillation may resemble the oscillation of a slow-rising polar crown filament in the pre-eruption phase, detected by Isobe & Tripathi (2006). However, our observation is very different, as we see low-amplitude steady oscillation in contrast with large-amplitude growing oscillation in both the coronal and chromospheric observational channels. Also, the oscillation period detected by Isobe & Tripathi (2006) was about two hours, and the polarization was found to be horizontal.

This work is supported by the European Research Council under the *SeismoSun* Research Project No. 321141, STFC consolidated grant ST/L000733/1, and the BK21 plus program through the National Research Foundation funded by the Ministry of Education of Korea (V.M.N.), and by the KASI basic research funds (S.K. and K.C.). The SDO data were (partly) provided by the Korea Data Center (KDC) for SDO in cooperation with NASA, which is supported by the “Development of Korea Space Weather Research Center” project of the Korea Astronomy and Space Science Institute (KASI). This research was

supported by the NRF of Korea Grant funded by the Ministry of Education (NRF-2013R1A1A2058409).

REFERENCES

- Arregui, I., Andries, J., Van Doorselaere, T., Goossens, M., & Poedts, S. 2007, *A&A*, **463**, 333
- Aschwanden, M. J., Fletcher, L., Schrijver, C. J., & Alexander, D. 1999, *ApJ*, **520**, 880
- Boerner, P., Edwards, C., Lemen, J., et al. 2011, *SoPh*, **275**, 41
- Cargill, P. J., Chen, J., & Garren, D. A. 1994, *ApJ*, **423**, 854
- De Moortel, I., & Nakariakov, V. M. 2012, *RSPTA*, **370**, 3193
- Goossens, M., Van Doorselaere, T., Soler, R., & Verth, G. 2013, *ApJ*, **768**, 191
- Hershaw, J., Foullon, C., Nakariakov, V. M., & Verwichte, E. 2011, *A&A*, **531**, A53
- Hindman, B. W., & Jain, R. 2014, *ApJ*, **784**, 103
- Isobe, H., & Tripathi, D. 2006, *A&A*, **449**, L17
- Karami, K., & Bahari, K. 2012, *ApJ*, **757**, 186
- Koutchmy, S., Zhugzhda, I. D., & Locans, V. 1983, *A&A*, **120**, 185
- Krall, J., Chen, J., Duffin, R. T., Howard, R. A., & Thompson, B. J. 2001, *ApJ*, **562**, 1045
- Kupriyanova, E. G., Melnikov, V. F., & Shibasaki, K. 2013a, *PASJ*, **65**, 3
- Kupriyanova, E. G., Melnikov, V. F., & Shibasaki, K. 2013b, *SoPh*, **284**, 559
- Lemen, J. R., Title, A. M., Akin, D. J., et al. 2011, *SoPh*, **275**, 17
- Luna, M., Terradas, J., Oliver, R., & Ballester, J. L. 2009, *ApJ*, **692**, 1582
- Nakariakov, V. M., & Ofman, L. 2001, *A&A*, **372**, L53
- Nakariakov, V. M., Ofman, L., Deluca, E. E., Roberts, B., & Davila, J. M. 1999, *Sci*, **285**, 862
- Nisticò, G., Nakariakov, V. M., & Verwichte, E. 2013, *A&A*, **552**, A57
- Ofman, L. 2009, *ApJ*, **694**, 502
- Ofman, L., & Aschwanden, M. J. 2002, *ApJL*, **576**, L153
- Shanmugaraju, A., Moon, Y.-J., Cho, K.-S., et al. 2010, *ApJ*, **708**, 450
- Soler, R., Oliver, R., & Ballester, J. L. 2009, *ApJ*, **693**, 1601
- Srivastava, A. K., & Goossens, M. 2013, *ApJ*, **777**, 17
- Terradas, J., Arregui, I., Oliver, R., et al. 2008, *ApJ*, **679**, 1611
- Terradas, J., & Goossens, M. 2012, *A&A*, **548**, A112
- Török, T., Kliem, B., & Titov, V. S. 2004, *A&A*, **413**, L27
- Van Doorselaere, T., Brady, C. S., Verwichte, E., & Nakariakov, V. M. 2008, *A&A*, **491**, L9
- Verth, G., & Erdélyi, R. 2008, *A&A*, **486**, 1015
- Verwichte, E., Foullon, C., & Nakariakov, V. M. 2006a, *A&A*, **449**, 769
- Verwichte, E., Foullon, C., & Nakariakov, V. M. 2006b, *A&A*, **452**, 615
- Wang, T., Ofman, L., Davila, J. M., & Su, Y. 2012, *ApJL*, **751**, L27
- Wang, T. J., & Solanki, S. K. 2004, *A&A*, **421**, L33
- White, R. S., Verwichte, E., & Foullon, C. 2012, *A&A*, **545**, A129